

# Reconstruction-based Multi-Normal Prototypes Learning for Weakly Supervised Anomaly Detection

Zhijin Dong<sup>1</sup>, Hongzhi Liu<sup>1,\*</sup>, Boyuan Ren<sup>1</sup>, Weimin Xiong<sup>1</sup>, Zhonghai Wu<sup>1</sup>

<sup>1</sup>Peking University

zhijindong@pku.edu.cn, liuhz@pku.edu.cn, rby\_tj@stu.pku.edu.cn, wmxiong@pku.edu.cn, wuzh@pku.edu.cn

## Abstract

Anomaly detection is a crucial task in various domains. Most of the existing methods assume the normal sample data clusters around a single central prototype while the real data may consist of multiple categories or subgroups. In addition, existing methods always assume all unlabeled data are normal while they inevitably contain some anomalous samples. To address these issues, we propose a reconstruction-based multi-normal prototypes learning framework that leverages limited labeled anomalies in conjunction with abundant unlabeled data for anomaly detection. Specifically, we assume the normal sample data may satisfy multi-modal distribution, and utilize deep embedding clustering and contrastive learning to learn multiple normal prototypes to represent it. Additionally, we estimate the likelihood of each unlabeled sample being normal based on the multi-normal prototypes, guiding the training process to mitigate the impact of contaminated anomalies in the unlabeled data. Extensive experiments on various datasets demonstrate the superior performance of our method compared to state-of-the-art techniques.

## 1 Introduction

Anomaly detection aims to identify samples that deviate significantly from the general data distribution, known as anomalies or outliers (Jiang et al. 2023). These anomalies often indicate potential problems or noteworthy events that require attention (Pang et al. 2021). The significance of anomaly detection spans a variety of critical domains, such as network security (Estévez-Pereira, Fernández, and Novoa 2020), Internet of Thing (IoT) security (Bulla and Birje 2022), and financial fraud detection (Popat and Chaudhary 2018). In each of these areas, effective anomaly detection methods are essential due to the substantial impact of anomalies.

In real-world scenarios, obtaining labeled data for anomaly detection is often challenging and costly (Jiang et al. 2023, 2024). Consequently, fully-supervised anomaly detection is impractical. While unsupervised methods bypass the need for extensive labeling, they struggle to achieve optimal performance without knowing what true anomalies look like. This limitation frequently results in the misidentification of noisy or irrelevant data points as anomalies (Pang

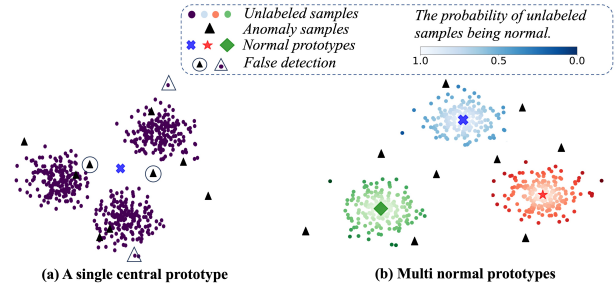


Figure 1: Motivations of multi-normal prototypes learning.

et al. 2023). To address these challenges, **weakly supervised anomaly detection** methods have emerged (Pang, Shen, and van den Hengel 2019; Ruff et al. 2020; Zhou et al. 2021; Xu et al. 2023b). These methods leverage a small portion of labeled anomalous data in conjunction with a large amount of unlabeled data, primarily composed of normal instances. This kind of approach is particularly significant in practical applications where we can only label a small fraction of anomalies.

However, existing anomaly detection methods still face two major challenges. First, most of the existing anomaly detection methods (Ruff et al. 2018a, 2020; Pang, Shen, and van den Hengel 2019) assume that normal data clusters around a single central prototype. However, real-world data often consists of multiple categories or subgroups (Fu, Zhang, and Fan 2024), making this assumption overly simplistic, as shown in Figure 1. Second, existing methods always assume all unlabeled data are normal while they inevitably contain some anomalous samples. Due to the assumption, many studies (Zhou et al. 2021; Fu, Zhang, and Fan 2024; Pang, Shen, and van den Hengel 2019) directly employ large amounts of unlabeled data as inliers for model training to identify the distribution of normal data patterns. These methods are vulnerable to the presence of occasional anomalies (i.e., anomaly contamination) within the unlabeled data, and the detection accuracy rapidly declines as the proportion of mixed-in anomalies increases (Pang et al. 2023; Xu et al. 2023b).

To address the problems stated above, we propose a reconstruction-based multi-normal prototype learning framework for weakly supervised anomaly detection. Dif-

\*Corresponding author.

ferent from existing reconstruction-based anomaly detection methods (Zhou et al. 2021), we treat the normal samples and anomalous samples differently during the latent representation learning with consideration of the likelihood of each unlabeled sample being normal. To better estimate the likelihood of normal and detect anomalies, we propose to learn multiple normal prototypes in the latent space with deep embedding clustering and contrastive learning. Finally, we compute a comprehensive anomaly score with consideration of both the information of sample reconstruction and multiple normal prototypes.

The main contributions of this paper can be summarized as follows:

- We propose a novel anomaly detection framework that combines reconstruction learning with multi-normal prototype learning. Extensive experiments across various datasets demonstrate that our method outperforms state-of-the-art techniques.
- We propose to build multiple normal prototypes with deep embedding clustering and contrastive learning to better model the distribution of normal data for anomaly detection.
- We propose to estimate and take into consideration the likelihood of each unlabeled sample being normal during model training, which can enhance resistance to anomaly contamination and more effectively detect unseen anomaly classes combined with previous designs.

## 2 Related Work

### 2.1 Anomaly Detection Based on Prototype Learning

One-class classification methods (Ruff et al. 2018b) are a fundamental category of traditional anomaly detection techniques. These methods are trained solely on normal data and identify anomalies by detecting deviations from a central prototype. Examples include One-Class SVM (OC-SVM) (Schölkopf et al. 1999), Support Vector Data Description (SVDD) (Tax and Duin 2004), Deep SVDD (Ruff et al. 2018a), and DeepSAD (Ruff et al. 2020), all of which assume that normal samples cluster around a single prototype in feature space, with anomalies located at the periphery. However, some studies have shown that normal data frequently consists of multiple categories or subgroups (Fu, Zhang, and Fan 2024), rendering a single prototype insufficient. To address these limitations, multi-prototype learning approaches have been developed to better represent the diversity within normal data, thereby enhancing anomaly detection capabilities. This concept has been applied across various domains, such as video anomaly detection (Park, Noh, and Ham 2020), image anomaly detection (Huang, Kang, and Wu 2024), and time series analysis (Li, Jentsch, and Müller 2023). These advancements highlight the potential of multi-prototype learning, particularly in the context of tabular data for weakly supervised anomaly detection.

### 2.2 Weakly Supervised Anomaly Detection

Weakly supervised anomaly detection has emerged as a solution to the limitations of purely unsupervised methods,

which struggle to identify what anomalies look like due to the lack of labeled examples (Pang et al. 2023). In weakly supervised settings, a small number of labeled anomalies are combined with a large amount of unlabeled data to enhance detection performance. Existing weakly supervised methods face notable challenges. Many rely heavily on large amounts of unlabeled data to identify normal data patterns, making them susceptible to contamination by occasional anomalies within the unlabeled dataset (Zhou et al. 2021; Ruff et al. 2020). This lack of effective mechanisms to mitigate the impact of these anomalies can significantly degrade detection performance, with accuracy declining rapidly as the proportion of mixed-in anomalies increases (Zhou et al. 2021; Fu, Zhang, and Fan 2024).

## 3 Methodology

### 3.1 Task Definition

In the context of weakly supervised anomaly detection, we are given a dataset  $\mathcal{X} = \{x_i\}_{i=1}^{N+K}$ , which contains two disjoint sets,  $\mathcal{X}_U$  and  $\mathcal{X}_A$ . Here,  $\mathcal{X}_U = \{x_i\}_{i=1}^N$  represents a large set of unlabeled samples, and  $\mathcal{X}_A = \{x_i\}_{i=N+1}^{N+K}$  (where  $K \ll N$ ) denotes a small set of labeled anomaly samples. Our objective is to learn a scoring function  $\phi : \mathcal{X} \rightarrow \mathbb{R}$  that assigns anomaly scores to each data instance, with the larger value of  $\phi(x_i)$  indicating a higher likelihood of  $x_i$  being an anomaly.

### 3.2 Overview of Our Method

To detect anomalies in a weakly supervised setting, we propose a novel approach combining reconstruction learning and multi-normal prototype learning, as illustrated in Figure 2. Our method consists of three main components: 1) **The Reconstruction Learning Module** aims to guide the latent representation learning with differentiated treatment to reconstruction errors of normal and anomalous samples; 2) **The Multi-Normal Prototypes Learning Module** aims to model the distribution of normal data better and utilizes deep embedding clustering and contrastive learning to build multiple normal prototypes for anomaly detection; 3) **The Unified Anomaly Scoring Module** aims to compute a comprehensive anomaly score with consideration of both the information of sample reconstruction and multiple normal prototypes. The detailed implementation of each component is described below.

### 3.3 Reconstruction Learning Module

This module serves two primary purposes: 1) transforming the data into a latent space to capture the essential features of samples; and 2) differentiating between normal and anomalous samples through reconstruction errors.

First, we employ an encoder-decoder structure for reconstruction learning. The encoder function  $\psi$  maps an input  $x_i \in \mathbb{R}^D$  to a latent representation  $z_i \in \mathbb{R}^H$ :

$$z_i = \psi(x_i; \Theta_\psi) \quad (1)$$

The decoder function  $\psi'$  maps the hidden representation  $z_i$  back to a reconstruction  $\hat{x}_i \in \mathbb{R}^D$  of the original input:

$$\hat{x}_i = \psi'(z_i; \Theta_{\psi'}) \quad (2)$$

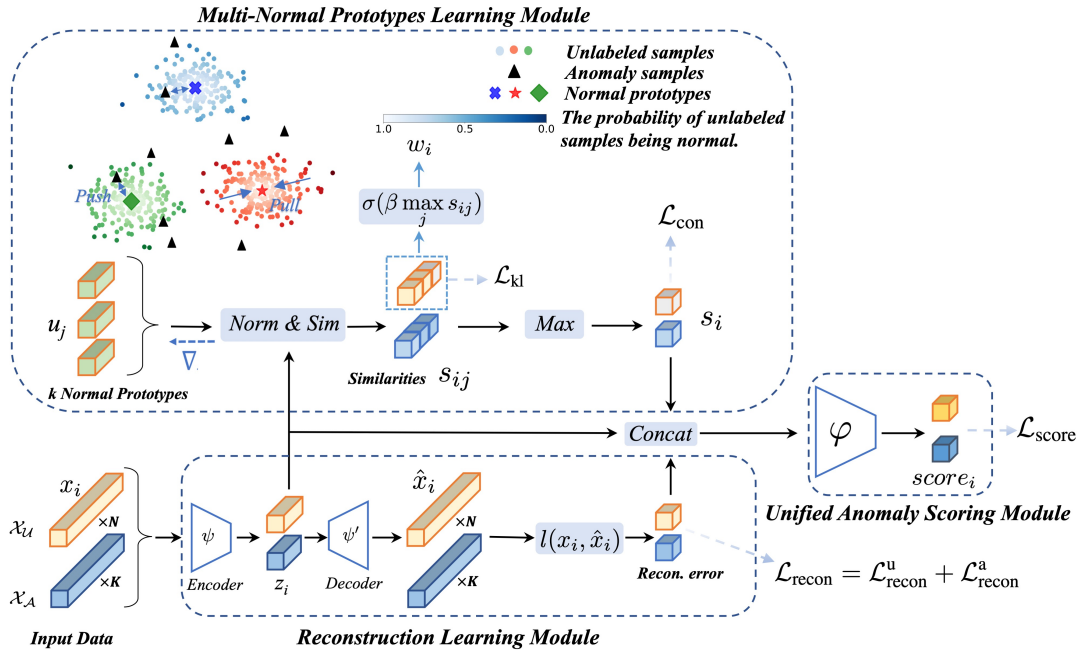


Figure 2: Overview of the proposed model. The input  $x_i$  from a labeled anomaly set  $\mathcal{X}_A$  and an unlabeled set  $\mathcal{X}_U$  are represented by blue and yellow shades, respectively. The output  $score_i$  indicates the likelihood of a sample being an anomaly.

where  $\Theta_\psi$  and  $\Theta_{\psi'}$  are the parameters of the encoder and decoder neural networks, respectively.

Second, we specifically design a reconstruction loss for weakly supervised anomaly detection. On the one hand, we minimize the reconstruction error to ensure that the latent representations capture the most relevant characteristics of the normal data. For unlabeled samples, the reconstruction loss is defined as:

$$\mathcal{L}_{recon}^u = \mathbb{E}_{x_i \sim \mathcal{X}_U} [w_i l(x_i, \hat{x}_i)] \quad (3)$$

where  $l$  is a regression loss function like Mean Squared Error (MSE), and  $w_i$  indicates the probability of an unlabeled sample being normal, reducing the impact of anomaly contamination in the training process by assigning them lower weights. The next module will detail how  $w_i$  is derived.

On the other hand, to distinguish normal samples from anomalies, we apply a hinge loss (Cortes and Vapnik 1995) to ensure that normal samples have a lower reconstruction loss compared to anomalies, maintaining a sufficient margin  $m_1$ . Therefore, the reconstruction loss for labeled anomalies is defined as:

$$\mathcal{L}_{recon}^a = \mathbb{E}_{x_i \sim \mathcal{X}_A} [\max(0, m_1 - (l(x_i, \hat{x}_i) - L_{recon}^u))] \quad (4)$$

The overall reconstruction loss, combining the losses for both unlabeled data and labeled anomalies, is given by:

$$\mathcal{L}_{recon} = \mathcal{L}_{recon}^u + \mathcal{L}_{recon}^a \quad (5)$$

### 3.4 Multi-Normal Prototypes Learning Module

We assume the normal sample data may consist of multiple categories or subgroups and satisfy multi-modal distribution. Therefore, we propose to learn multiple prototypes

to represent the normal data. Specifically, we utilize deep embedding clustering and contrastive learning to learn multiple normal prototypes.

**Initialization and Similarity Calculation.** At the beginning of training, we initialize  $k$  normal prototypes by clustering normal data's latent representations from the pre-train Encoder following (Guo et al. 2017), denoted as  $\{u_j \in \mathbb{R}^H\}_{j=1}^k$ . During the model training and inference phases, we need to calculate the similarity between a given sample  $x_i$  and each prototype  $u_j$  to determine which category or subgroup the sample belongs to. Specifically, we assume the samples of each category or subgroup satisfy the Student's  $t$ -distribution, and calculate the similarity between sample  $x_i$  and prototype  $u_j$  as follows:

$$s_{ij} = Sim(z_i; \Theta_{\{u_j\}_{j=1}^k}) = \left(1 + \frac{\|z_i - u_j\|^2}{\alpha}\right)^{-\frac{\alpha+1}{2}} \quad (6)$$

where  $z_i$  denotes the latent representation of sample  $x_i$ ,  $\alpha$  is the degree of freedom of the Student's  $t$ -distribution,  $\Theta_{\{u_j\}_{j=1}^k}$  is the parameters of the multi-normal prototypes, consistent with the neural network parameters that can be optimized via backpropagation. To ensure consistency and stability during training, both the normal prototype  $u_j$  and the latent representation  $z_i$  are normalized before calculating the similarity.

**Weights of Unlabeled Samples.** In our anomaly detection framework, the weights of unlabeled samples are crucial for adjusting the influence of each sample during the training process. The weights, which represent the probability of unlabeled samples being normal, help to mitigate the contamination effect of anomalies within unlabeled data. We define

the weight  $w_i$  for an unlabeled sample  $x_i$  based on its maximum similarity to any normal prototype:

$$w_i = \sigma(\beta \max_j s_{ij}) \quad (7)$$

where  $\sigma$  is the sigmoid activation function, and  $\beta$  is a scaling parameter that adjusts the sensitivity of the similarity scores.

Unlabeled samples with higher similarity to normal prototypes are assigned greater weights, increasing their influence in the loss function associated with unlabeled data and focusing the model on preserving the characteristics of normal samples. Conversely, unlabeled samples with lower similarity scores, likely to be anomalies, receive smaller weights, reducing their impact on the model’s learning process. This strategy effectively minimizes the adverse effects of anomaly contamination, ensuring the model remains sensitive to the features of normal behavior while suppressing the noise introduced by unlabeled anomalies.

**Clustering and Contrastive Learning.** To enhance the accuracy of anomaly detection, we propose to construct multiple normal prototypes to capture the diversity within normal data. However, initial prototypes may not fully represent the underlying structure of the normal data. Therefore, we refine these prototypes through a two-step process.

First, recognizing that the relationship between normal samples and multiple normal prototypes aligns with an unsupervised clustering problem, we employ Deep Embedding Clustering (Xie, Girshick, and Farhadi 2016), which utilizes deep neural networks to simultaneously learn feature representations and cluster assignments. This process involves optimizing a KL divergence loss for unlabeled samples:

$$\mathcal{L}_{kl}(P \parallel Q) = \sum_i \sum_j p_{ij} \log \frac{p_{ij}}{q_{ij}} \quad (8)$$

where

$$q_{ij} = \frac{s_{ij}}{\sum_{j'} s_{ij'}}, \quad f_j = \sum_i q_{ij}, \quad p_{ij} = \frac{q_{ij}^2 / f_j}{\sum_{j'} q_{ij'}^2 / f_{j'}}$$

This loss function encourages the prototypes to align closely with the central tendencies of the clusters formed by the normal data, ensuring that the learned prototypes accurately reflect the true structure of the normal data distribution.

Second, to solidify the distinction between normal data and anomalous data, we introduce a contrastive learning approach. Our goal is to ensure that normal samples exhibit high similarity to at least one of the refined normal prototypes while maintaining low similarity for anomalous samples across all prototypes. This separation is enforced through a contrastive loss function:

$$\mathcal{L}_{con} = -\log \sigma(\mathbb{E}_{x_i \sim \mathcal{X}_U} [w_i \max_j s_{ij}] - \mathbb{E}_{x_i \sim \mathcal{X}_A} [\max_j s_{ij}]) \quad (9)$$

where  $w_i$  ensures that unlabeled anomalies do not achieve high similarity to any normal prototypes. Through this contrastive learning process, normal samples are encouraged to cluster around one of the central prototypes in the latent space, while anomalous samples are pushed to the periphery, far from any normal prototype. This method ensures a clear

and robust separation between normal and anomalous data, significantly enhancing the effectiveness of the anomaly detection framework.

Finally, we combine the Clustering Loss (8) with Contrastive Loss (9) to get the overall loss for this module:

$$\mathcal{L}_{np} = \mathcal{L}_{con} + \mathcal{L}_{kl} \quad (10)$$

Dataset Name	Abbr.	$D$	$N$	$\delta(\%)$
UNSW-NB15 Dos	DoS	196	109,353	15.0
UNSW-NB15 Rec	Rec	196	106,987	13.1
UNSW-NB15 Backdoor	bac	196	95329	2.4
UNSW-NB15 Analysis	Ana	196	95677	2.8
IoT-23 C&C	C&C	24	31,619	17.8
IoT-23 Attack	Attack	24	29,815	12.8
IoT-23 DDoS	DDoS	24	26037	0.1
IoT-23 Okiru	Okiru	24	26164	0.6
Fraud Detection	Fraud	29	284,807	0.2
Vehicle Claims	VC	306	268,255	21.2
Vehicle Insurance	VI	148	15,420	6.0
MAGIC Gamma	Gamma	10	19,020	35.2
Census Income	Census	500	299,285	6.2
Pendigits	Pendigits	16	6,870	2.3
Bank Marketing	Bank	62	41,188	11.3

Table 1: Overview of Datasets.  $D$  and  $N$  denote data dimension and size, respectively.  $\delta$  indicates the anomaly ratio.

### 3.5 Unified Anomaly Scoring Module

To detect anomalies with consideration of both the reconstruction error  $e_i = l(x_i, \hat{x}_i)$  and the multi-normal prototype information, we design a unified anomaly scoring module. Inspired by the residual network (He et al. 2016), we also take the latent representation  $z_i$  of the given sample  $x_i$  as the input. In summary, the concatenated vector forms the input to the unified anomaly score evaluator  $\varphi$  to get an anomaly score:

$$score_i = \varphi(\text{cat}(e_i, z_i, s_i); \Theta_\varphi) \quad (11)$$

where  $s_i = \max_j s_{ij}$  is the maximum similarity to any normal prototype,  $\Theta_\varphi$  denotes the trainable parameters of the unified anomaly score evaluator, which is composed of a multi-layer perceptron with a sigmoid activation function at the final layer.

We aim for the anomaly scores to be close to 1 for anomalous samples and close to 0 for normal samples. Thus, we design the following loss function:

$$\mathcal{L}_{score} = \mathbb{E}_{x_i \sim \mathcal{X}_U} [w_i \cdot l(score_i, 0)] + \mathbb{E}_{x_i \sim \mathcal{X}_A} [l(score_i, 1)] \quad (12)$$

where the weights  $w_i$  are applied to mitigate the influence of anomalies in the unlabeled data, focusing the model’s learning on the more reliable, normal-like samples.

### 3.6 Training and Inference

**Training.** Our model is trained in an end-to-end manner using mini-batches consisting of  $b_u$  unlabeled samples and  $b_a$  labeled anomalies. For each mini-batch, we compute

Data	Ours	RoSAS	PReNet	DevNet	DeepSAD	FeaWAD	DeepIForest	DeepSVDD	IForest
DoS	<b>0.946</b> ±0.004	0.742±0.024	0.695±0.006	<u>0.906</u> ±0.022	0.489±0.184	0.571±0.310	0.414±0.005	0.263±0.041	0.148±0.007
Rec	<b>0.851</b> ±0.008	0.770±0.011	<u>0.787</u> ±0.006	0.763±0.023	0.695±0.051	0.210±0.095	0.163±0.008	0.196±0.060	0.104±0.004
Bac	<u>0.870</u> ±0.005	0.543±0.023	0.461±0.006	<b>0.878</b> ±0.011	0.509±0.036	0.221±0.174	0.247±0.025	0.143±0.075	0.046±0.003
Ana	<b>0.910</b> ±0.008	0.556±0.045	0.451±0.016	<u>0.854</u> ±0.063	0.249±0.076	0.268±0.235	0.223±0.018	0.141±0.067	0.064±0.007
C&C	<b>0.519</b> ±0.011	0.367±0.026	0.378±0.003	<u>0.419</u> ±0.056	0.146±0.001	0.247±0.061	0.145±0.002	0.181±0.024	0.180±0.004
Attack	<b>0.964</b> ±0.012	<u>0.961</u> ±0.014	0.906±0.008	0.954±0.010	0.428±0.441	0.635±0.381	0.162±0.004	0.276±0.256	0.261±0.013
DDoS	<b>0.252</b> ±0.202	0.071±0.088	0.003±0.002	0.047±0.049	0.059±0.024	0.043±0.056	0.117±0.014	0.081±0.034	<u>0.146</u> ±0.040
Okiru	<b>0.518</b> ±0.003	<u>0.191</u> ±0.079	0.008±0.001	0.144±0.090	0.105±0.009	0.126±0.109	0.010±0.001	0.012±0.016	0.019±0.001
Fraud	<b>0.679</b> ±0.021	0.433±0.029	0.351±0.099	<u>0.512</u> ±0.152	0.098±0.054	0.130±0.130	0.382±0.020	0.021±0.022	0.139±0.034
VC	<b>0.697</b> ±0.005	0.497±0.006	0.322±0.006	<u>0.654</u> ±0.014	0.189±0.010	0.256±0.037	0.261±0.004	0.234±0.038	0.255±0.019
VI	<b>0.106</b> ±0.012	0.079±0.003	0.070±0.009	<u>0.093</u> ±0.005	0.058±0.001	0.082±0.006	0.062±0.005	0.063±0.004	0.064±0.002
Gamma	<u>0.780</u> ±0.014	0.726±0.018	<b>0.782</b> ±0.005	0.749±0.013	0.577±0.163	0.569±0.040	0.698±0.007	0.437±0.021	0.644±0.008
Census	<b>0.392</b> ±0.023	0.309±0.018	0.150±0.007	<u>0.391</u> ±0.011	0.105±0.026	0.183±0.086	0.074±0.002	0.054±0.015	0.077±0.003
Pendigits	<b>0.856</b> ±0.042	<u>0.852</u> ±0.020	0.065±0.039	0.766±0.060	0.686±0.073	0.396±0.308	0.234±0.037	0.073±0.088	0.274±0.025
Bank	<b>0.286</b> ±0.010	0.245±0.016	0.146±0.012	<u>0.246</u> ±0.030	0.122±0.010	0.127±0.027	0.233±0.006	0.198±0.048	<u>0.283</u> ±0.011
<b>Average</b>	<b>0.642</b> ± 0.025	0.489 ± 0.028	0.372 ± 0.015	<u>0.558</u> ± 0.041	0.301 ± 0.077	0.271 ± 0.137	0.228 ± 0.011	0.158 ± 0.054	0.180 ± 0.012
<b>P-value</b>	-	<0.0001	0.0001	0.0002	<0.0001	<0.0001	<0.0001	<0.0001	<0.0001
DoS	<b>0.978</b> ±0.003	0.835±0.049	0.795±0.006	<u>0.963</u> ±0.005	0.603±0.189	0.755±0.210	0.787±0.015	0.506±0.065	0.525±0.029
Rec	<b>0.972</b> ±0.003	0.922±0.010	0.922±0.001	<u>0.951</u> ±0.001	0.820±0.057	0.611±0.207	0.457±0.025	0.510±0.098	0.410±0.021
Bac	<b>0.976</b> ±0.003	0.882±0.029	0.751±0.016	<u>0.972</u> ±0.006	0.660±0.033	0.717±0.246	0.904±0.002	0.641±0.152	0.727±0.009
Ana	<b>0.995</b> ±0.001	0.936±0.038	0.782±0.022	<u>0.987</u> ±0.005	0.440±0.102	0.798±0.099	0.916±0.004	0.564±0.122	0.781±0.022
C&C	<b>0.733</b> ±0.003	0.723±0.001	<u>0.730</u> ±0.003	0.729±0.008	0.427±0.002	0.568±0.057	0.426±0.007	0.492±0.039	0.495±0.004
Attack	<b>0.999</b> ±0.000	<u>0.998</u> ±0.002	0.992±0.000	<u>0.998</u> ±0.000	0.410±0.481	0.815±0.281	0.643±0.010	0.397±0.461	0.820±0.013
DDoS	<b>0.822</b> ±0.163	0.427±0.066	0.521±0.067	0.466±0.079	0.673±0.042	0.494±0.124	<u>0.783</u> ±0.087	0.504±0.067	0.780±0.002
Okiru	<u>0.960</u> ±0.001	0.951±0.014	0.579±0.028	<b>0.961</b> ±0.005	0.946±0.012	0.896±0.109	0.692±0.026	0.676±0.323	0.845±0.009
Fraud	<u>0.964</u> ±0.006	0.896±0.015	0.867±0.032	<b>0.967</b> ±0.015	0.744±0.105	0.655±0.280	0.962±0.002	0.533±0.094	0.957±0.003
VC	<b>0.774</b> ±0.005	0.702±0.007	0.559±0.004	<u>0.754</u> ±0.005	0.373±0.016	0.544±0.029	0.559±0.005	0.451±0.037	0.561±0.026
VI	<b>0.693</b> ±0.031	0.578±0.013	0.528±0.040	<u>0.639</u> ±0.016	0.476±0.008	0.606±0.030	0.486±0.030	0.502±0.015	0.501±0.012
Gamma	<u>0.845</u> ±0.008	0.807±0.014	<b>0.846</b> ±0.003	0.837±0.004	0.663±0.156	0.700±0.057	0.773±0.008	0.536±0.017	0.727±0.007
Census	<b>0.896</b> ±0.003	0.781±0.026	0.574±0.007	<u>0.895</u> ±0.004	0.429±0.059	0.703±0.172	0.614±0.010	0.463±0.078	0.627±0.015
Pendigits	<u>0.986</u> ±0.007	<b>0.989</b> ±0.002	0.710±0.121	0.971±0.014	0.823±0.113	0.761±0.214	0.949±0.008	0.770±0.202	0.953±0.005
Bank	<b>0.701</b> ±0.008	0.676±0.015	0.552±0.025	0.677±0.019	0.470±0.022	0.516±0.087	0.666±0.003	0.541±0.036	<u>0.691</u> ±0.012
<b>Average</b>	<b>0.886</b> ± 0.016	0.807 ± 0.020	0.714 ± 0.025	<u>0.851</u> ± 0.012	0.597 ± 0.093	0.676 ± 0.147	0.708 ± 0.016	0.539 ± 0.120	0.693 ± 0.013
<b>P-value</b>	-	0.0002	0.0001	0.0009	<0.0001	<0.0001	<0.0001	<0.0001	<0.0001

Table 2: Performance comparison of different methods. The upper section presents AUC-PR (primary metric) and the lower section shows AUC-ROC. The best results are highlighted in bold and the second-best results are underlined.

three losses:  $L_{recon}$ ,  $L_{np}$ , and  $L_{score}$ , as defined by equation (3), (10), and (12), respectively. To effectively balance these three losses dynamically, we utilize a technique known as Dynamic Averaging, inspired by (Liu, Johns, and Davison 2018). The total loss is calculated as follows:

$$\mathcal{L}_{total} = w_1 \mathcal{L}_{recon} + w_2 \mathcal{L}_{np} + w_3 \mathcal{L}_{score} \quad (13)$$

where  $w_1$ ,  $w_2$ , and  $w_3$  are updated per epoch based on the rate of descent of the corresponding losses.

All parameters ( $\Theta_{\{\psi, \psi'\}}$ ,  $\Theta_{\{u_j\}_{j=1}^k}$ ,  $\Theta_{\varphi}$ ) are jointly optimized with respect to the total loss ensuring a comprehensive and integrated training process for the model.

**Inference.** During the inference phase, each data instance  $x_i$  is passed through the Reconstruction Learning Module to obtain its latent representation  $z_i$  and reconstruction error  $e_i$ . The Multi-Normal Prototypes Learning Module then calculates the similarity between the latent representation and the normal prototypes, selecting the maximum similarity score  $s_i$ . The three features are fed into the anomaly score evaluator  $\varphi$  to compute an anomaly score for each instance.

## 4 Experiments

### 4.1 Experimental Setup

**Datasets** This section outlines the datasets used in our experiments, covering a broad range of scenarios across domains like network security, Internet of Thing (IoT) security, financial fraud detection, and others. All 15 datasets are summarized in Table 1, providing robust benchmarks for evaluating anomaly detection methods with their diverse scenarios and varying anomaly ratios.

**Baseline Methods** This section outlines the algorithms that are most comparable to our proposed method. These algorithms are grouped into two categories based on their supervision level: 1) **Weakly supervised algorithms**, such as RoSAS (Xu et al. 2023b), PReNet (Pang et al. 2023), DevNet (Pang, Shen, and van den Hengel 2019), DeepSAD (Ruff et al. 2020), and FeaWAD (Zhou et al. 2021), leverage limited labeled data alongside a larger set of unlabeled data, offering a direct comparison to our approach; 2) **Un-supervised algorithms** like DeepIForest (Xu et al. 2023a), DeepSVDD (Ruff et al. 2018a), and iForest (Liu, Ting, and

Zhou 2012), operate without any labeled data, offering a baseline to assess the benefits of incorporating even minimal labeled data in anomaly detection.

**Evaluation Metrics** We use the Area Under the Precision-Recall Curve (AUC-PR) as the primary evaluation metric, complemented by the Area Under the Receiver Operating Characteristic Curve (AUC-ROC). AUC-PR is ideal for imbalanced datasets, emphasizing correct anomaly detection while minimizing false positives and negatives. Both metrics range from 0 to 1, with higher values indicating better performance. Results are averaged over 5 runs, and the paired Wilcoxon signed-rank test (Woolson 2008) is used to validate the significance of our findings.

**Implementation Details** We scale each feature to  $[0, 1]$  via min-max normalization. We use the Adam optimizer with a learning rate of  $5 \times 10^{-3}$  and weight decay of  $5 \times 10^{-4}$ . The hidden representation dimension  $H$  is set to 8, and the hyperparameters are configured as follows: batch sizes  $b_u = 128$ ,  $b_a = 32$ ; margin  $m_1 = 0.02$ ; Student’s  $t$ -distribution degree of freedom  $\alpha = 1$ ; and similarity scaling parameter  $\beta = 1$ . The number of normal prototypes is determined via clustering analysis on the unlabeled samples. Implementation of the compared methods is based on the DeepOD framework (Xu et al. 2023a).

## 4.2 Performance Comparison

In our experiments, we evaluate the performance of our proposed anomaly detection method across multiple datasets with a fixed labeled anomaly ratio of 1.0% for each dataset. The labeled anomaly ratio is defined as the proportion of anomalies in the training dataset that are labeled. Table 2 shows the performance of different methods on the fifteen benchmark datasets. Our method consistently outperformed other approaches, achieving the highest average scores in both AUC-PR and AUC-ROC metrics, with statistically significant improvements with over 99.9% confidence. Specifically, in terms of AUC-PR, our method achieved the best results on 13 of the 15 datasets, and was the second-best on the remaining two, closely approaching the top results. The average AUC-PR of our method was 0.642, which is significantly higher than other methods. Similarly, for the AUC-ROC metric, our method achieved an average of 0.886, surpassing all other methods. The statistical validation further confirmed that the improvements brought by our method are significant, providing robust and reliable anomaly detection performance in weakly supervised settings. Besides, the weakly supervised algorithms, such as our method, RoSAS, and DevNet, perform significantly better than all unsupervised algorithms on almost all datasets. This confirms that with the appropriate use of a few labeled anomaly samples, we can get better anomaly detection performance.

## 4.3 Effects of More or Less Labeled Anomalies

This experiment aims to examine the effects of Labeled Anomaly Ratios on the model’s effectiveness in detecting anomalies, helping us understand the trade-off between supervision level and detection performance. From Figure 3, it is evident that our method consistently achieves the best

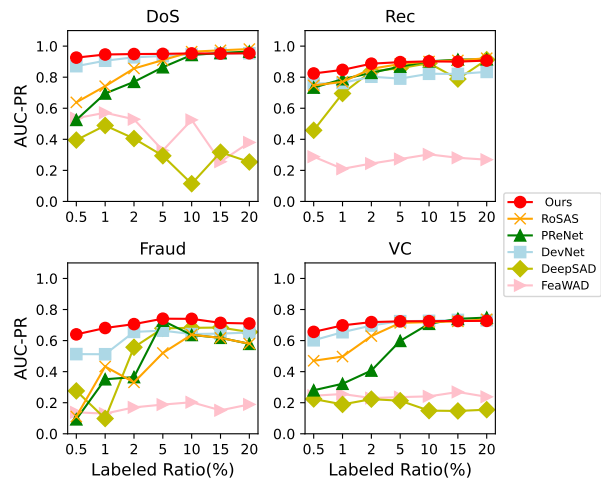


Figure 3: Effects of varying the ratios of labeled anomalies.

performance across nearly all Labeled Anomaly Ratios. Specifically, as the Labeled Anomaly Ratios decrease, our method’s performance degrades more slowly and maintains relatively high detection performance, while other methods exhibit a significant decline in most datasets. On the other hand, from the perspective of anomaly contamination, as the proportion of labeled anomalies decreases, the proportion of unlabeled anomalies contaminating the unlabeled data increases. Figure 3 shows that, unlike other methods, our method’s detection performance declines more slowly as the anomaly contamination ratio increases, maintaining a relatively good detection performance. This demonstrates the robustness of our model against anomaly contamination.

## 4.4 Detection Performance on Unseen Anomalies

A crucial aspect of an effective anomaly detection system is its ability to generalize from known anomalies to detect previously unseen ones. This capability is essential for maintaining robustness in dynamic environments where new types of anomalies may emerge. To evaluate our method’s performance on unseen anomalies, we constructed several experimental datasets using the UNSW-NB15 dataset, which contains four types of anomalies: DoS, Rec, Ana, and Bac. In each experiment, two types of anomalies were selected: one used exclusively in the test set (unseen) and the other included in the training and validation sets (seen). This setup resulted in 12 different experimental datasets.

The results are presented in Table 3, showing the AUC-PR scores for different methods across various combinations of seen and unseen anomaly types. Our method achieved the highest average AUC-PR of 0.765, significantly outperforming other methods by more than 20%. The statistical confidence level for this improvement exceeds 99.0%. This experiment demonstrates that our method can effectively generalize from known anomalies to detect previously unseen ones, maintaining strong detection performance and robustness in dynamic environments.

Seen	Unseen	Ours	RoSAS	PRENet	DevNet	DeepSAD	FeaWAD	DeepIForest	DeepSVDD	IForest
Rec	DoS	<b>0.824</b> ±0.041	0.515±0.042	0.354±0.045	0.512±0.067	0.311±0.092	0.279±0.146	0.654±0.013	0.311±0.083	0.212±0.013
Ana	DoS	<b>0.904</b> ±0.011	0.710±0.053	0.546±0.019	0.882±0.015	0.415±0.080	0.651±0.180	0.659±0.014	0.370±0.121	0.248±0.036
Bac	DoS	<b>0.868</b> ±0.009	0.654±0.060	0.538±0.012	0.867±0.009	0.461±0.069	0.658±0.245	0.668±0.024	0.312±0.077	0.256±0.030
DoS	Rec	<b>0.681</b> ±0.033	0.653±0.022	0.389±0.040	0.566±0.066	0.324±0.104	0.274±0.145	0.161±0.004	0.199±0.042	0.097±0.007
Ana	Rec	<b>0.534</b> ±0.105	0.250±0.026	0.176±0.004	0.469±0.047	0.257±0.063	0.281±0.038	0.210±0.011	0.275±0.080	0.133±0.005
Bac	Rec	<b>0.699</b> ±0.057	0.566±0.048	0.478±0.037	0.535±0.031	0.375±0.011	0.297±0.120	0.213±0.007	0.197±0.054	0.124±0.007
DoS	Ana	<b>0.844</b> ±0.015	0.537±0.010	0.493±0.004	0.843±0.016	0.266±0.110	0.477±0.243	0.116±0.009	0.097±0.043	0.034±0.004
Rec	Ana	<b>0.586</b> ±0.033	0.180±0.019	0.082±0.013	0.198±0.051	0.138±0.067	0.077±0.047	0.253±0.020	0.137±0.068	0.056±0.004
Bac	Ana	0.785±0.020	0.417±0.034	0.365±0.009	<b>0.828</b> ±0.021	0.324±0.062	0.244±0.243	0.263±0.006	0.231±0.114	0.069±0.010
DoS	Bac	<b>0.865</b> ±0.018	0.615±0.016	0.578±0.007	0.851±0.013	0.313±0.127	0.525±0.267	0.105±0.006	0.085±0.048	0.021±0.001
Rec	Bac	<b>0.735</b> ±0.023	0.320±0.055	0.169±0.049	0.166±0.021	0.153±0.059	0.095±0.036	0.250±0.030	0.226±0.126	0.045±0.009
Ana	Bac	<b>0.857</b> ±0.004	0.415±0.045	0.334±0.021	0.815±0.068	0.289±0.079	0.238±0.239	0.243±0.016	0.153±0.038	0.051±0.007
<b>Average</b>		<b>0.765</b> ± 0.031	0.486 ± 0.036	0.375 ± 0.022	0.628 ± 0.035	0.302 ± 0.077	0.341 ± 0.162	0.316 ± 0.013	0.216 ± 0.075	0.112 ± 0.011
<b>P-value</b>		-	0.0005	0.0005	0.0068	0.0005	0.0005	0.0005	0.0005	0.0005

Table 3: Detection of unseen anomalies, with performance measured by AUC-PR. The "Seen" indicates the anomaly type included in the training and validation sets, while the "Unseen" indicates the anomaly type only included in the test set.

Method	Average AUC-PR	P-value
w/o $\mathcal{L}_{recon}$	0.622 ± 0.038	0.0008
w/o $\mathcal{L}_{np}$	0.618 ± 0.022	0.0038
w/o $w_i$	0.602 ± 0.042	<0.0001
w/o Decoder	0.611 ± 0.052	<0.0001
w/o MNP	0.566 ± 0.021	<0.0001
Full Model	<b>0.642</b> ± 0.025	-

Table 4: Results of ablation study.

## 4.5 Ablation Study

We conducted an ablation study to assess the impact of each component in our model, as shown in Table 4. The results demonstrate that the full model achieves the highest AUC-PR of 0.642. Specifically, excluding the reconstruction loss or the normal prototype loss, deleting weight  $w_i$ , and removing the Decoder included reconstruction error all resulted in decreased AUC-PR values. Notably, the most significant performance degradation occurred when the multi-normal prototypes (MNP) were excluded, with the AUC-PR dropping to 0.566, highlighting the essential role of multi-prototype learning in our model.

## 4.6 Sensitivity Analysis

In this section, we investigate the effects of varying the number of normal prototypes. As shown in Figure 4 (illustrating four representative datasets), most datasets achieve better results with multiple prototypes, confirming our hypothesis that normal data is multi-categorical. In the Rec dataset, prototype count has little effect, indicating lower sensitivity. However, in the C&C and Census datasets, the choice of prototype number is crucial—too many or too few prototypes can significantly degrade performance. In the Bank dataset, although performance fluctuates with the number of prototypes, it consistently outperforms using a single prototype.

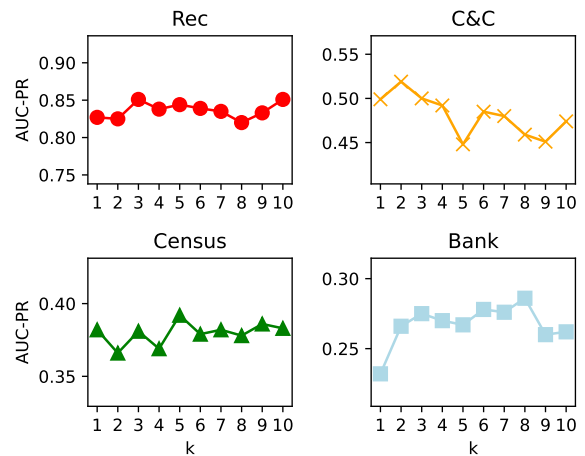


Figure 4: Effects of varying the number of normal prototypes

## 5 Conclusions

In conclusion, our proposed anomaly detection method demonstrates significant improvements over existing techniques by effectively leveraging a small amount of labeled anomaly data alongside a large amount of unlabeled data. Our method's robustness to anomaly contamination and its ability to generalize to unseen anomalies make it highly suitable for real-world applications across various domains. Future work could explore extending our method to other types of data, such as images, to further validate its versatility and effectiveness. For the reconstruction learning component, we could also consider using more advanced variants like Variational AutoEncoders (VAEs) to enhance feature extraction capabilities.

## References

Bulla, C.; and Birje, M. N. 2022. *Anomaly Detection in Industrial IoT Applications Using Deep Learning Approach*, 127–147. Cham: Springer International Publishing.

- Cortes, C.; and Vapnik, V. 1995. Support-Vector Networks. *Machine Learning*, 20(3): 273–297.
- Estévez-Pereira, J. J.; Fernández, D.; and Novoa, F. J. 2020. Network Anomaly Detection Using Machine Learning Techniques. *Proceedings*, 54(1).
- Fu, D.; Zhang, Z.; and Fan, J. 2024. Dense Projection for Anomaly Detection. *Proceedings of the AAAI Conference on Artificial Intelligence*, 38(8): 8398–8408.
- Guo, X.; Gao, L.; Liu, X.; and Yin, J. 2017. Improved deep embedded clustering with local structure preservation. In *IJCAI*, 1753–1759.
- He, K.; Zhang, X.; Ren, S.; and Sun, J. 2016. Deep residual learning for image recognition. In *Proceedings of the IEEE conference on computer vision and pattern recognition*, 770–778.
- Huang, C.; Kang, Z.; and Wu, H. 2024. A Prototype-Based Neural Network for Image Anomaly Detection and Localization. *Neural Processing Letters*, 56(3).
- Jiang, M.; Hou, C.; Zheng, A.; Han, S.; Huang, H.; Wen, Q.; Hu, X.; and Zhao, Y. 2024. ADGym: design choices for deep anomaly detection. In *Proceedings of the 37th International Conference on Neural Information Processing Systems*, NIPS '23. Red Hook, NY, USA: Curran Associates Inc.
- Jiang, M.; Hou, C.; Zheng, A.; Hu, X.; Han, S.; Huang, H.; He, X.; Yu, P. S.; and Zhao, Y. 2023. Weakly supervised anomaly detection: A survey. *arXiv preprint arXiv:2302.04549*.
- Li, B.; Jentsch, C.; and Müller, E. 2023. Prototypes as Explanation for Time Series Anomaly Detection. *arXiv:2307.01601*.
- Liu, F. T.; Ting, K. M.; and Zhou, Z.-H. 2012. Isolation-Based Anomaly Detection. *ACM Trans. Knowl. Discov. Data*, 6(1).
- Liu, S.; Johns, E.; and Davison, A. J. 2018. End-To-End Multi-Task Learning With Attention. *2019 IEEE/CVF Conference on Computer Vision and Pattern Recognition (CVPR)*, 1871–1880.
- Pang, G.; Shen, C.; Cao, L.; and Hengel, A. V. D. 2021. Deep learning for anomaly detection: A review. *ACM computing surveys (CSUR)*, 54(2): 1–38.
- Pang, G.; Shen, C.; Jin, H.; and van den Hengel, A. 2023. Deep Weakly-supervised Anomaly Detection. In *Proceedings of the 29th ACM SIGKDD Conference on Knowledge Discovery and Data Mining*, KDD '23, 1795–1807.
- Pang, G.; Shen, C.; and van den Hengel, A. 2019. Deep Anomaly Detection with Deviation Networks. In *Proceedings of the 25th ACM SIGKDD International Conference on Knowledge Discovery & Data Mining*, KDD '19, 353–362.
- Park, H.; Noh, J.; and Ham, B. 2020. Learning Memory-guided Normality for Anomaly Detection. *arXiv:2003.13228*.
- Popat, R. R.; and Chaudhary, J. 2018. A Survey on Credit Card Fraud Detection Using Machine Learning. In *2018 2nd International Conference on Trends in Electronics and Informatics (ICOEI)*, 1120–1125.
- Ruff, L.; Görnitz, N.; Deecke, L.; Siddiqui, S. A.; Vandermeulen, R. A.; Binder, A.; Müller, E.; and Kloft, M. 2018a. Deep One-Class Classification. In *Proceedings of the 35th International Conference on Machine Learning, ICML 2018*, 4390–4399.
- Ruff, L.; Vandermeulen, R.; Goernitz, N.; Deecke, L.; Siddiqui, S. A.; Binder, A.; Müller, E.; and Kloft, M. 2018b. Deep One-Class Classification. In *Proceedings of the 35th International Conference on Machine Learning*, Proceedings of Machine Learning Research, 4393–4402.
- Ruff, L.; Vandermeulen, R. A.; Görnitz, N.; Binder, A.; Müller, E.; Müller, K.-R.; and Kloft, M. 2020. Deep Semi-Supervised Anomaly Detection. In *International Conference on Learning Representations*.
- Schölkopf, B.; Williamson, R. C.; Smola, A.; Shawe-Taylor, J.; and Platt, J. 1999. Support vector method for novelty detection. *Advances in neural information processing systems*, 12.
- Tax, D.; and Duin, R. 2004. Support Vector Data Description. *Machine Learning*, 54: 45–66.
- Woolson, R. F. 2008. *Wilcoxon Signed-Rank Test*, 1–3. John Wiley & Sons, Ltd.
- Xie, J.; Girshick, R.; and Farhadi, A. 2016. Unsupervised deep embedding for clustering analysis. In *Proceedings of the 33rd International Conference on International Conference on Machine Learning - Volume 48*, ICML'16, 478–487.
- Xu, H.; Pang, G.; Wang, Y.; and Wang, Y. 2023a. Deep Isolation Forest for Anomaly Detection. *IEEE Transactions on Knowledge and Data Engineering*, 35(12): 12591–12604.
- Xu, H.; Wang, Y.; Pang, G.; Jian, S.; Liu, N.; and Wang, Y. 2023b. RoSAS: Deep semi-supervised anomaly detection with contamination-resilient continuous supervision. *Information Processing & Management*, 60(5): 103459.
- Zhou, Y.; Song, X.; Zhang, Y.; Liu, F.; Zhu, C.; and Liu, L. 2021. Feature Encoding With Autoencoders for Weakly Supervised Anomaly Detection. *IEEE Transactions on Neural Networks and Learning Systems*, 33: 2454–2465.